Engineering Fracture Mechanics Vol. 28, No. 5/6, pp. 741–760, 1987
Printed in Great Britain.

0013-7944/87 $3.00 + .00

STUDY ON CRACKED PLATES, SHELLS AND THREE DIMENSIONAL BODIES

LIU CHUNTU and LI YINGZHI
Institute of Mechanics, Chinese Academy of Sciences, China

Abstract—This paper presents a summary of the authors' recent work in following areas: (1) The stress–strain fields at crack tip in Reissner's plate. (2) The calculations of the stress intensity factors in finite size plates. (3) The stress–strain fields at crack tip in Reissner's shell. (4) The calculations of the stress intensity factors and bulging coefficients in finite size spherical shells. (5) The stress–strain fields along crack tip in three dimensional body with surface crack. (6) The calculation of stress intensity factors in a plate with surface crack.

1. INTRODUCTION

THE STUDY of cracked bending plates, shells and three dimensional bodies is one of the fundamental problems in engineering. The problem is of considerable importance in many areas, such as aerospace industry, chemical industry, etc. Having reviewed the recent research work in this subject, the authors proposed following research line: (1) In order to avoid the defect of classical theory, the Reissner's theory, taking into account the transversal shear deformation, is used to deal with cracked plate and shell problem. (2) So-called "Local-Global Analysis" is used to deal with cracked plate, shell and three dimensional body problem. As local analysis, we search for the stress–strain fields at crack tip, which provide a better foundation for global numerical analysis.

2. STUDY ON CRACKED PLATE BENDING FRACTURE PROBLEM

In earlier literature the classical theory was used to deal with a cracked bending plate problem[1, 2]. In recent years more investigators began to study the problem with Reissner's theory. In refs [3, 4], the singularity of Reissner's plate was studied. In ref. [5] the expansion of stress–strain fields at crack tip for symmetric case were obtained. In refs [6, 7] the stress intensity factors K_{II} and K_{III} in an infinite plate were calculated using an integral transformation method. For a finite size plate in bending, in refs [3–11] the stress intensity factors for mode I were calculated using Reissner's theory. Recently, authors proposed a general solution of stress–strain fields at a crack tip including mode I, mode II and mode III, calculated the stress intensity factors for mixed mode in a finite size plate[12–14] as well.

(a) *The stress–strain fields at crack tip*

Based on Reissner's theory, the governing equations could be expressed in terms of three generalized displacements ψ_x, ψ_y and w as follows:

$$D\left(\frac{\partial^2\psi_x}{\partial x^2}+\frac{1-\nu}{2}\cdot\frac{\partial^2\psi_x}{\partial y^2}+\frac{1+\nu}{2}\cdot\frac{\partial^2\psi_y}{\partial x\,\partial y}\right)+C\left(\frac{\partial w}{\partial x}-\psi_x\right)=0, \tag{2.1}$$

$$D\left(\frac{1+\nu}{2}\cdot\frac{\partial^2\psi_x}{\partial x\,\partial y}+\frac{1-\nu}{2}\frac{\partial^2\psi_y}{\partial x^2}+\frac{\partial^2\psi_y}{\partial y^2}\right)+C\left(\frac{\partial w}{\partial y}-\psi_y\right)=0, \tag{2.2}$$

$$C\left(\frac{\partial^2 w}{\partial x^2}+\frac{\partial^2 w}{\partial y^2}-\frac{\partial\psi_x}{\partial x}-\frac{\partial\psi_x}{\partial y}\right)+p=0 \tag{2.3}$$

where $D=\dfrac{Eh^3}{12(1-\nu^2)}$ is bending stiffness,

$C=\dfrac{5}{6}Gh$ is shearing stiffness.

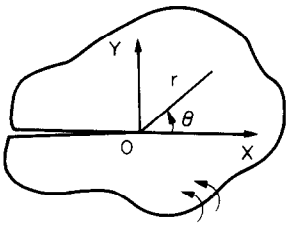

Fig. 2.1. A plate with semi-infinite crack.

The boundary conditions are (Fig. 2.1). When

$$\theta = \pm\pi$$

$$M_\theta = M_{r\theta} = Q_\theta = 0. \tag{2.4}$$

We introduced two displacement functions F and f:

$$\phi_x = \frac{\partial F}{\partial x} + \frac{\partial f}{\partial y}, \qquad \phi_y = \frac{\partial F}{\partial y} - \frac{\partial f}{\partial x}. \tag{2.5}$$

Substituting eq. (2.5) into (2.1), (2.2) we have

$$\frac{\partial}{\partial x}[D\nabla^2 F + C(W - F)] + \frac{\partial}{\partial y}\left[\frac{D}{2}(1-\nu)\nabla^2 f - Cf\right] = 0, \tag{2.6}$$

$$\frac{\partial}{\partial y}[D\nabla^2 F + C(W - F)] - \frac{\partial}{\partial x}\left[\frac{D}{2}(1-\nu)\nabla^2 f - Cf\right] = 0. \tag{2.7}$$

This is the Cauchy–Riemann equation, from which it follows that

$$\frac{D}{2}(1-\nu)\nabla^2 f - Cf + \mathrm{i}[D\nabla^2 F + C(W - F)] = C\Phi(x + \mathrm{i}y). \tag{2.8}$$

Separating the real part and imaginary part in eq. (2.8), we have

$$\nabla^2 f - 4k^2 f = 4k^2 \operatorname{Re}\Phi, \tag{2.9}$$

$$W = F - \frac{D}{C}\nabla^2 F + \operatorname{Im}\Phi, \tag{2.10}$$

where

$$4k^2 = \frac{2C}{D(1-\nu)} = \frac{10}{h^2}.$$

Substituting eqs (2.5), (2.10) into eq. (2.3), we have

$$D\nabla^2\nabla^2 F = P. \tag{2.11}$$

For a cracked plate, the bending fracture problems are reduced to two equations, (2.9), (2.11) in terms of F and f with the boundary conditions.

The function $\Phi(x+iy)$ could be expanded in series

$$\Phi(x+iy)=\sum_{\mu}(\beta\mu+i\alpha\mu)\Phi^{\mu}=\sum_{\mu}(\beta\mu+i\alpha\mu)\Phi^{\mu}(\cos\mu\theta+i\sin\mu\theta). \tag{2.12}$$

The solution of eqs (2.9), (2.11) could be expressed in the sum of a particular solution and the general solution of the corresponding homogeneous equations.

The particular solution could be chosen as follows

$$f_1=-\mathrm{Re}\,\Phi, \qquad F_1=0. \tag{2.13}$$

The homogeneous equation corresponding to eq. (2.9) is

$$\nabla^2 f_0-4k^2 f_0=0. \tag{2.14}$$

When $p=0$, from eq. (2.11), we have

$$D\nabla^2\nabla^2 F=0. \tag{2.15}$$

Equation (2.15) is a biharmonic equation, we have

$$\begin{aligned}F(r,\theta)&=\sum_{\lambda}r^{\lambda+1}F(\theta)\\&=\sum_{\lambda}r^{\lambda+1}[K_\lambda\cos(\lambda-1)\theta+L_\lambda\sin(\lambda-1)\theta+M_\lambda\cos(\lambda+1)\theta+N_\lambda\sin(\lambda+1)\theta].\end{aligned} \tag{2.16}$$

Equation (2.14) is a Helmholtz equation, function f_0 could be expressed in modified Bessel functions. From the condition of finite strain energy, we should drop out the modified Bessel function of second kind and f_0 could be expressed in modified Bessel functions of first kind $I_\lambda(2kr)$ only.

For symmetric case

$$f_\lambda=\sin\lambda\theta I_\lambda(2kr)=\sin\lambda\theta\sum_{m=0,1,\ldots}\frac{k^{2m}r^{\lambda+2m}}{m!\phi(\lambda,m)}. \tag{2.17}$$

For anti-symmetric case

$$f^*_\lambda=\cos\lambda\theta I_\lambda(2kr)=\cos\lambda\theta\sum_{m=0,1,\ldots}\frac{k^{2m}r^{\lambda+2m}}{m!\phi(\lambda,m)}, \tag{2.18}$$

where

$$\begin{aligned}&\phi(\lambda,m)=(\lambda+1)(\lambda+2)\ldots(\lambda+m) && (\text{for } m\geqslant 1),\\&\phi(\lambda,m)=1 && (\text{for } m=0).\end{aligned}$$

To determine the coefficients of expansion, it is convenient that the general solution of eq. (2.14) is expressed in the following linear combination.

$$f_0=\sum_{\lambda}\sum_{n=0,1,\ldots}(A_{\lambda-1+2n}f_{\lambda-1+2n}+B_{\lambda-1+2n}f^*_{\lambda-1+2n}). \tag{2.19}$$

Substituting eqs (2.16), (2.19) into eqs (2.14), (2.15), the linear equations whose unknowns

are the coefficients of the expansions could be obtained. In order to satisfy these equations, we let

$$\lambda = \pm\frac{n}{2}, \qquad n = 0, 1, 2, \ldots \tag{2.20}$$

With the condition of finite strain energy, λ should be positive. By using the boundary conditions, the relations between coefficients in eigenfunction expansion could be found. With the expression of F and f known, the expressions of ψ_r, ψ_θ and w as well as M_r, M_θ, $M_{r\theta}$, Q_r, Q_θ could be obtained.

(b) *Numerical examples*

Example 1. *Infinite plate with uniform bending moment.* This problem was studied by Hartranft and Sih[2]. The stress intensity factor is

$$K_1(g) = \frac{12g}{h^3}\phi(1)M\sqrt{\pi a}. \tag{2.21}$$

The maximum value takes place at $z = h/2$.

$$K_1 = \frac{6M}{h^2}\phi_{(1)}\sqrt{\pi a}. \tag{2.21'}$$

In order to simulate the infinite plate, the plate semilength L should be larger than $20a$. The graph and results are shown in Figs 2.2 and 2.3, respectively.

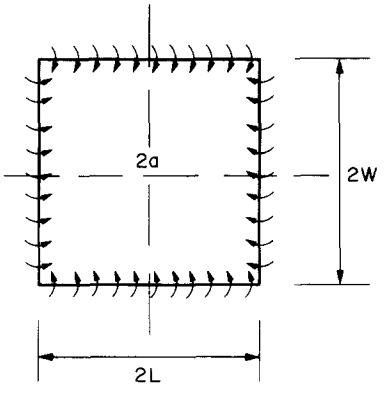

Fig. 2.2. A cracked plate with uniform bending moment.

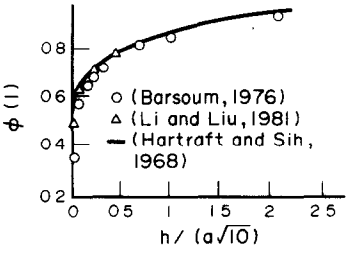

Fig. 2.3. Comparison of authors' solution with others.

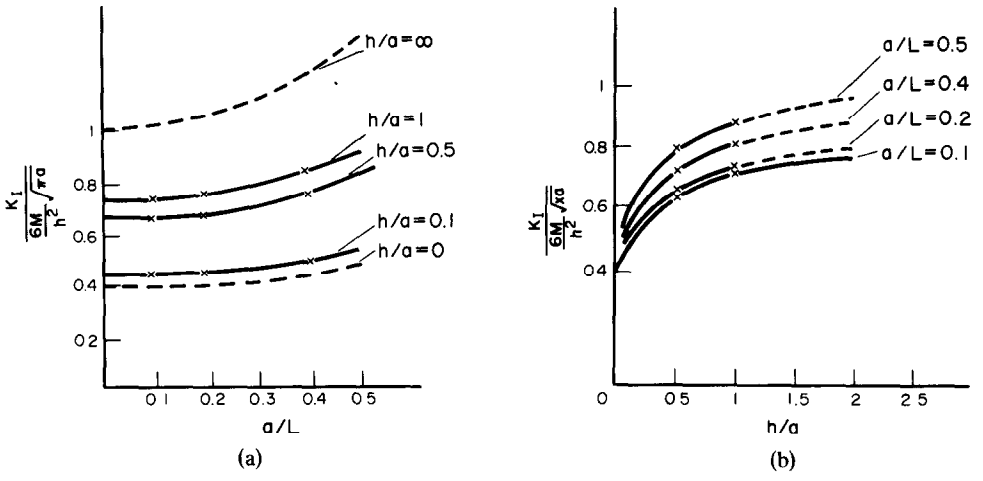

Fig. 2.4. (a) Variation of stress intensity factors with plate width. (b) Variation of stress intensity factors with plate thickness.

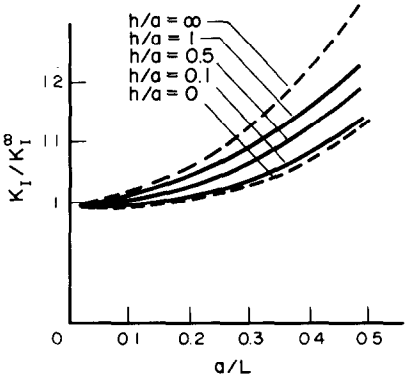

Fig. 2.5. Finite size coefficient.

Example 2. *Finite plate with uniform bending moment*[11]. In order to investigate the variation of stress intensity factors of finite plate with different thickness and width, the stress intensity factors for $a/L = 0.1$, 0.2, 0.4 and 0.5 are calculated. The results are shown in Fig. 2.4(a, b) respectively. The finite size coefficient K_I/K_I^∞ are shown in Fig. 2.5, where K_I^∞ denotes K_I for infinite case.

Example 3. *The effect of boundary conditions on the stress intensity factors*[11]. In order to compare the effects of different boundary conditions on the stress intensity factors, the calculations of the simple supported plate and free plate are carried out. The results are shown in Fig. 2.6. In the calculation the bending moment is taken as 1 kg-cm/cm and $h/a = 1$.

Example 4. *Cracked plate with uniform twist moment*[13, 14]. This is a mixed mode (Fig. 2.7). For infinite case, this problem was studied by Delale[7] using an integral transformation method. The dimensionless stress intensity factors k_2, k_3 are

$$k_2 = \frac{K_{II}(h/2)}{(6M/h^2)\sqrt{\pi a}}, \tag{2.22}$$

$$k_3 = \frac{K_{III}(0)}{(6M/h^2)\sqrt{\pi a}}, \tag{2.23}$$

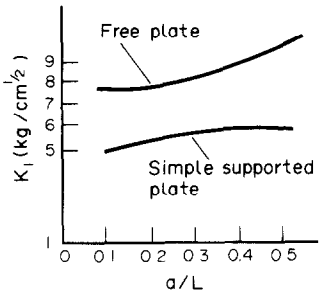

Fig. 2.6. Effect of boundary conditions.

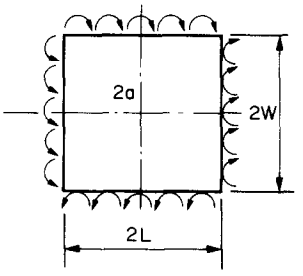

Fig. 2.7. A cracked plate with uniform twist moment.

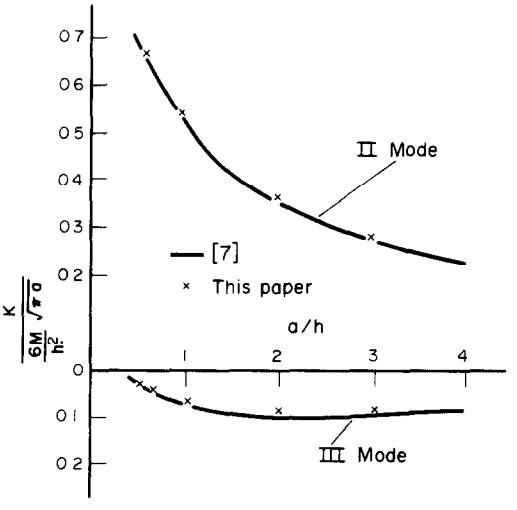

Fig. 2.8. Comparison of authors' solution with others ($a/L \to 0$).

where $K_{II}(h/2)$, $K_{III}(0)$ are stress intensity factors for mode II and mode III, respectively. The maximum stress intensity factor for mode II takes place at the plate surface, for mode III at the middle of the section. In order to simulate the infinite plate, we let $2L = 100a$, the solution compares favourably with that in ref. [7] (see Fig. 2.8).

For a finite size plate, the variation of stress intensity factors with width and thickness is shown in Fig. 2.9. The finite size coefficients k_2/k_2^∞, k_3/k_3^∞ are shown in Figs 2.10, 2.11, where k_2^∞, k_3^∞ denote k_2, k_3 for infinite case.

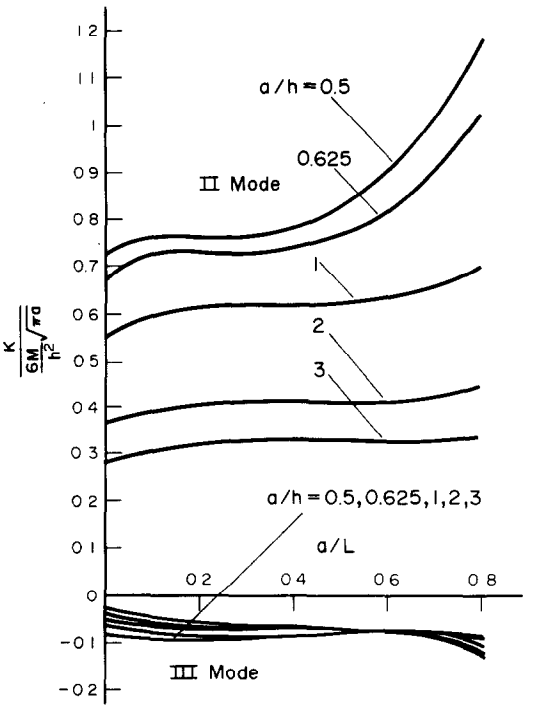

Fig. 2.9. Variation of stress intensity factors with width and thickness.

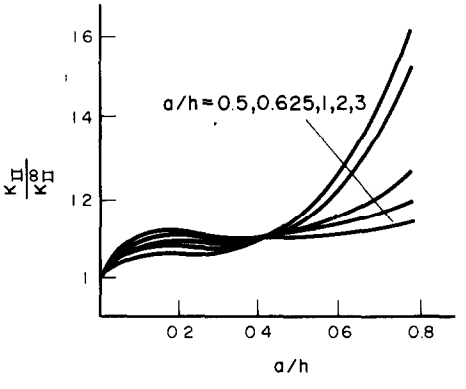

Fig. 2.10. The finite size coefficient k_2/k_2^{∞}.

(c) *J-integral in Reissner's plate*

Similar to J-integral in plane fracture problem, a J_R integral in Reissner's plate was proposed[15].

$$J_R = \int_c U\,\mathrm{d}y + \int_c \left(-Q_n \frac{\partial W}{\partial x} + \bar{M}_x \frac{\partial \psi_x}{\partial x} + \bar{M}_y \frac{\partial \psi_y}{\partial x}\right) \mathrm{d}S, \tag{2.24}$$

where U denotes the unit strain energy, $\bar{M}_x$, $\bar{M}_y$ denote boundary moments, Q_n denotes boundary shear.

The relation between J_R and stress intensity factors is

$$J_R = \frac{h}{8E}(K_I^2 + K_{II}^2) + \frac{4h}{15G} K_{III}^2. \tag{2.25}$$

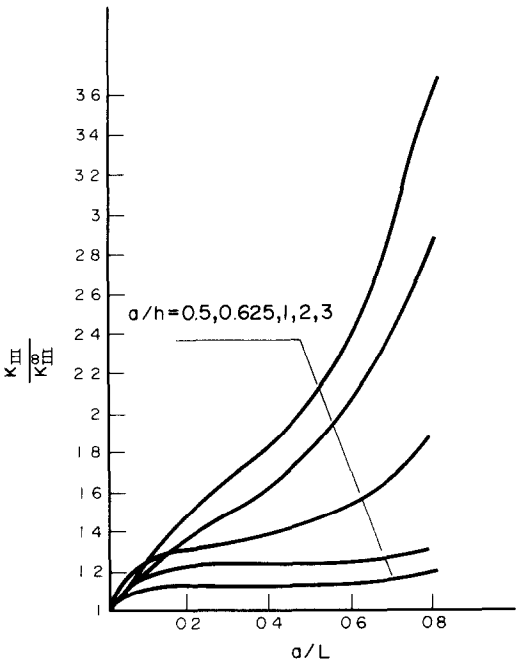

Fig. 2.11. The finite size coefficient k_3/k_3^{∞}.

J_R can be used in approximate analysis of stress intensity factors. It also can be used as a parameter in elastic–plastic fracture analysis.

3. STUDY ON CRACKED SPHERICAL SHELL FRACTURE PROBLEM

Since curvature exists in shells, extension and bending are coupled, which makes the problem very difficult. In the earlier literature the classical theory was used[16–18]. In recent years, the Reissner's shell theory was used and a ten order differential equation was derived[19]. Since the problem is complicated, only the first term of the expansion was given[20–22]. In order to calculate stress intensity factors (especially for mixed mode), the authors proposed an expansion of the stress–strain fields at the crack tip including mode I, mode II and mode III, we also got some significant results in bulging coefficients[23–25].

(a) *The stress–strain fields at crack tip in a spherical shell*

A spherical shell containing a through crack is shown in Fig. 3.1 with the crack tip at the origin of the coordinates. The shallow shell theory, taking into account of shear deformation,

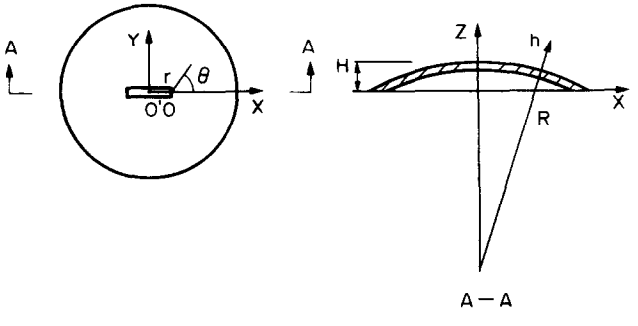

Fig. 3.1. A cracked spherical shell.

could be expressed as follows.

$$D\left(\frac{\partial^2\psi_x}{\partial x^2}+\frac{1-\nu}{2}\frac{\partial^2\psi_x}{\partial y^2}+\frac{1+\nu}{2}\frac{\partial^2\psi_y}{\partial x\,\partial y}\right)+C\left(\frac{\partial W}{\partial x}-\psi_x\right)=0, \tag{3.1}$$

$$D\left(\frac{1+\nu}{2}\frac{\partial^2\psi_x}{\partial x\,\partial y}+\frac{1-\nu}{2}\frac{\partial^2\psi_y}{\partial x^2}+\frac{\partial^2\psi_y}{\partial y^2}\right)+C\left(\frac{\partial W}{\partial y}-\psi_y\right)=0, \tag{3.2}$$

$$C\left(\frac{\partial^2 W}{\partial x^2}+\frac{\partial^2 W}{\partial y^2}-\frac{\partial\psi_x}{\partial x}-\frac{\partial\psi_y}{\partial y}\right)+k\nabla^2\varphi+q=0, \tag{3.3}$$

where k is the curvature, φ is the stress function

$$N_x=\frac{\partial^2\varphi}{\partial y^2},\qquad N_y=\frac{\partial^2\varphi}{\partial x^2},\qquad N_{xy}=-\frac{\partial^2\varphi}{\partial x\,\partial y}.$$

The compatibility equation is

$$\frac{1}{B}\nabla^2\nabla^2\varphi+k\nabla^2 W=0, \tag{3.4}$$

where B is the in-plate stiffness.

Introducing displacement functions F and f, let

$$\psi_x=\frac{\partial F}{\partial x}+\frac{\partial f}{\partial y},\qquad \psi_y=\frac{\partial F}{\partial y}-\frac{\partial f}{\partial x}. \tag{3.5}$$

Substituting eq. (3.5) into eqs (3.1), (3.2), we have

$$\begin{aligned}&\frac{\partial}{\partial x}[D\nabla^2F+C(W-F)]+\frac{\partial}{\partial y}\left[\frac{D}{2}(1-\nu)\nabla^2 f-Cf\right]=0,\\&\frac{\partial}{\partial y}[D\nabla^2F+C(W-F)]-\frac{\partial}{\partial x}\left[\frac{D}{2}(1-\nu)\nabla^2 f-Cf\right]=0.\end{aligned} \tag{3.6}$$

Equation (3.6) is a Cauchy–Riemann equation, from which it follows that

$$\frac{D}{2}(1-\nu)\nabla^2 f-Cf+\mathrm{i}[D\nabla^2F+C(W-F)]=C\Phi(x+\mathrm{i}y). \tag{3.7}$$

Separating the real part and imaginary part in eq. (3.7), we have

$$D\nabla^2F+C(W-F)=C\,\mathrm{Im}\,\Phi, \tag{3.8}$$

$$\frac{D}{2}(1-\nu)\nabla^2 f-Cf=C\,\mathrm{Re}\,\Phi. \tag{3.9}$$

From eq. (3.8), we have

$$W=F-\frac{D}{C}\nabla^2F+\mathrm{Im}\,\Phi. \tag{3.10}$$

Substituting eqs (3.5), (3.10) into eq. (3.3), we have

$$D\nabla^2\nabla^2F-k\nabla^2\varphi=q. \tag{3.11}$$

Substituting eq. (3.10) into eq. (3.4), we have

$$\frac{1}{B}\nabla^2\nabla^2\varphi + k\nabla^2 F - k\frac{D}{C}\nabla^2\nabla^2 F = 0. \tag{3.12}$$

The governing equations could be reduced to three eqs (3.9), (3.11) and (3.12) in terms of F, f and φ. The function f, which is similar to that in the bending plate case, is uncoupled. The functions F and φ should satisfy two four-order differential equations.

If $q = 0$, from eq. (3.11), (3.12), we have

$$\nabla^2\nabla^2\nabla^2 F - \frac{k^2 B}{C}\nabla^2\nabla^2 F + \frac{k^2 B}{D}\nabla^2 F = 0. \tag{3.13}$$

It can be proved that, function F in eq. (3.13) is the sum of three functions F_0, F_1 and F_2, which should satisfy the following equations respectively.

$$F = F_0 + F_1 + F_2, \tag{3.14}$$

$$\nabla^2 F_0 = 0, \tag{3.15}$$

$$\nabla^2 F_1 - 4\lambda_1^2 F_1 = 0, \tag{3.16}$$

$$\nabla^2 F_2 - 4\lambda_2^2 F_2 = 0, \tag{3.17}$$

where

$$4\lambda_1^2 = \frac{k^2 B}{2C} + \sqrt{\frac{k^4 B^2}{4C^2} - \frac{k^2 B}{D}}, \qquad 4\lambda_2^2 = \frac{k^2 B}{2C} - \sqrt{\frac{k^4 B^2}{4C^2} - \frac{k^2 B}{D}}.$$

With the F known, from eq. (3.11) the φ could be obtained.

$$\varphi = \varphi_0 + \frac{4D}{k}(\lambda_1^2 F_1 + \lambda_2^2 F_2), \tag{3.18}$$

where φ_0 is an harmonic function, which should satisfy $\nabla^2\varphi_0 = 0$.

From eq. (3.9), function f could be found as

$$f = f_0 - \mathrm{Re}\,\Phi. \tag{3.19}$$

f_0 should satisfy the following equation

$$\nabla^2 f_0 - 4\mu^2 f_0 = 0, \tag{3.20}$$

where

$$4\mu^2 = \frac{2C}{D(1-\nu)}.$$

The boundary conditions are when $\theta = \pm\pi$,

$$M_\theta = M_{r\theta} = Q_\theta = N_{r\theta} = N_\theta = 0. \tag{3.21}$$

The analytic function Φ could be expanded in series

$$\Phi(x + \mathrm{i}y) = \sum_\mu (\beta_\mu + \mathrm{i}\alpha_\mu) g^\mu = \sum_\mu (\beta_\mu + \mathrm{i}\alpha_\mu) r^\mu (\cos\mu\theta + 1\sin\mu\theta). \tag{3.22}$$

Harmonic function F_0 could also be expanded in series

$$F_0 = \sum_{\lambda} r^{\lambda+1}[K^{(0)}_{\lambda+1} \cos(\lambda+1)\theta + L^{(0)}_{\lambda+1} \sin(\lambda+1)\theta]. \tag{3.23}$$

Functions f_0, F_1 and F_2 should satisfy the eq. (3.20), (3.16), (3.17) respectively. These equations are Helmholtz's equations. Their solutions could be expressed in modified Bessel functions. With the condition of finite energy, we must drop out the modified Bessel functions of second kind. The functions f_0, F_1 and F_2 could then be expressed in modified Bessel functions of the first kind only.

Similar to the bending cracked plate problem, substituting the expansion f, F and φ into the boundary conditions eq. (3.21), the linear equations whose unknowns are the coefficients of the expansions could be established. From these equations, the relations between the coefficients in the eigenfunction expansion could be found. With the functions f, F and φ known, the generalized displacements and stress could be obtained.

(b) *Numerical examples*

Example 1. *Cracked spherical shell under bending.* For infinite shell case, this problem was studied by Sih and Hagendorf. For finite size shell case, we introduce $\lambda = \sqrt[4]{12(1-\nu)^2}a/\sqrt{Rh}$ as a curvature parameter.

The variation of stress intensity factors with a/L in a finite spherical shell is shown in Fig. 3.2.

When $\lambda = 0$, that is the case of flat plate, the numerical results approach theoretical values in ref. [4] with an error less than 1% as $a/L \to 0$, and also agree very well with the results for finite plate obtained in ref. [11]. When $\lambda > 0$, that is the case of shell, as $a/L \to 0$ the value of our results drops by almost 30% compared with the theoretical value. This can be explained in the following way. As we know, the spherical surface can not geometrically extend to infinity, when λ or a/R was given, the shell goes deeper and deeper as a/L decreases, and the assumptions for shallow shell theory are no longer valid. This indicates that the results obtained in ref. [20] are invalid for some ranges.

Example 2. *Pressurized spherical shell under different boundary conditions.* Considering a spherical cap of $L/R = \pi/4$ under uniform pressure q_0, stress intensity factors for different boundary conditions are given in Fig. 3.3. Compared with the value of stress intensity factors for free edge shell case, the value of stress intensity factors reduced by 16% for simple support shell case, and by 20% for fixed support shell case.

(c) *Bulging factor of spherical shell*

A formula of stress intensity factor of pressurized spherical shell was obtained by Folias[16]

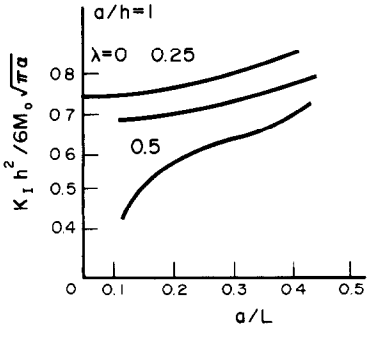

Fig. 3.2. The effect of finite size.

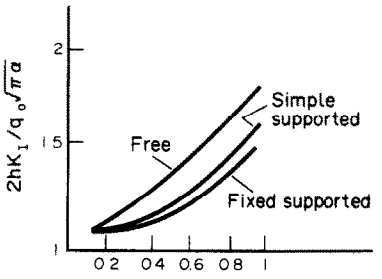

Fig. 3.3. The effect of boundary conditions.

using the Kirchoff classical thin shell theory, which can be expressed as follows:

$$K_I = M\sigma\sqrt{\pi a}, \tag{3.24}$$

where $\sigma = q_0 R/2h$ is the shell stress with q_0 as uniform pressure; M is bulging factor. Its approximate formula has the form:

$$M_\lambda = (1 + 0.59\lambda^2)^{1/2}. \tag{3.25}$$

In classical theory, M depends on the curvature parameter λ only. In Reissner's theory, a new parameter $\kappa = D/ca^2$ is introduced, taking into account shear stiffness. The numerical results of bulging factor are shown in Fig. 3.4. It is shown that for small values of κ, the values of our results agree well with the classical values, but depart from the classical values as κ increases.

Based on the results of calculation, an approximate formula is given as follows:

$$M(\lambda, \kappa) = M_\lambda(1 + 1.2\kappa^{1/3}\lambda\, e^{-\lambda}), \qquad \lambda < 2.2. \tag{3.26}$$

4. STUDY ON THREE DIMENSIONAL BODY WITH SURFACE CRACK

Since Irwin[26] first proposed an approximate solution of surface crack problem in 1962, many investigators have proposed miscellaneous methods to improve Irwin's solution. Smith *et al.*[27–30] used an alternating method, Rice–Levy[31] proposed a line spring model concept, Cruse used the boundary integral equation method, Nisitani *et al.*[32, 33] put forward a body force method and so on. The results of research work before 1972 were included in ref. [34].

In 1979 Newman and Raju[35] collected the results of thirteen investigators' research work and published their results of three dimensional finite element analysis by using near ten thousand freedoms[36, 37]. Their formulas have been adopted by ASTM E740-80 Standard[38].

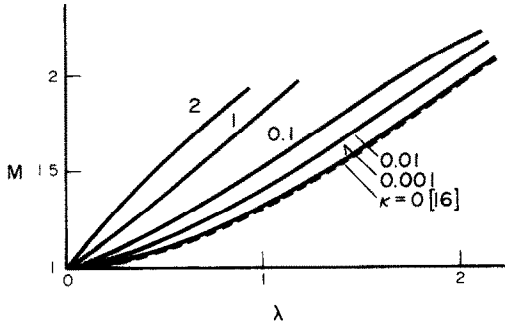

Fig. 3.4. Bulging factor of spherical shell.

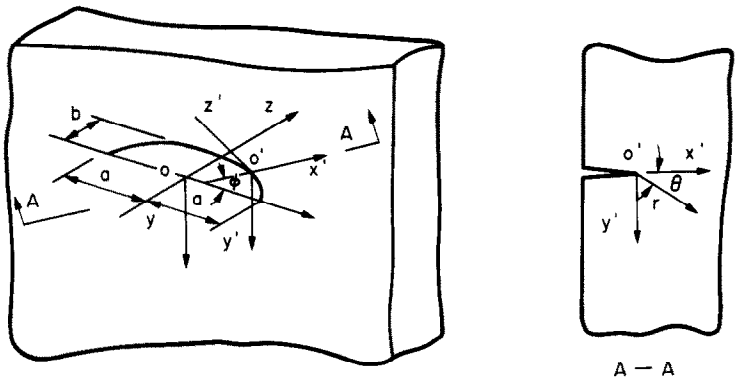

Fig. 4.1. Coordinate transformation.

In engineering practice, three dimensional finite method is one of efficient methods. However, it needs large computer storage and consumes long computer time. Furthermore, above research work almost deals with the mode I symmetrical case, because numerical calculation for mixed mode needs more accurate stress–strain modes. But so far, the research in stress–strain fields at surface crack is insufficient. Only the first term of stress strain fields was found, the whole fields are unclear. Therefore, it is important to search for the stress–strain fields along surface crack tip. It can provide a better foundation for numerical analysis.

(a) *Stress–strain fields at crack tip in three dimensional body with surface crack*

Consider a three dimensional body with a surface crack. Take the Cartesian coordinates as shown in Fig. 4.1 and denote the plane xOy as the front surface.

Let's introduce a special coordinate transformation with parameters γ, θ, φ. The new coordinate system can simplify the boundary condition, so that it can be represented as $\theta = \pm\pi$.

New coordinate system can be established in this way:

Let axis y' parallel to axis y, plane $x'Oz'$ move on plane xOz and the new original point O' move along the crack tip front. Axis $O'x'$ and $O'z'$ are the normal and tangent of the ellipse respectively. Denote the angle between axes $O'x'$ and Ox as φ, introduce polar coordinate γ, θ in plane $x'O'z'$. The new coordinate system with parameters γ, θ, φ could be established.

The relations between new and old coordinate systems are:

$$\begin{aligned} x &= \frac{a\cos\varphi}{(1-e^2\sin^2\varphi)^{1/2}} + r\cos\theta\cos\varphi, \\ y &= r\sin\theta, \\ z &= \frac{b^2\sin\varphi}{a(1-e^2\sin^2\varphi)^{1/2}} + r\cos\theta\sin\psi. \end{aligned} \tag{4.1}$$

From eq. (4.1) the gauge coefficients and Christoffel coefficients could be calculated, from which the three dimensional governing equations in curvilinear coordinate could be established.

$$\begin{aligned} &2(1-\nu)\left(\frac{\partial^2 u_r}{\partial r^2} + \frac{\partial u_r}{r\,\partial r} - \frac{u_r}{r^2}\right) + (1-2\nu)\frac{\partial^2 u_r}{r^2\,\partial\theta^2} + \frac{\partial^2 u_\theta}{r\,\partial r\,\partial\theta} - (3-4\nu)\frac{\partial u_\theta}{r^2\partial\theta} \\ &+ \frac{1}{\Phi}\left[\frac{\partial^2 u_\psi}{\partial r\,\partial\varphi} + 2(1-\nu)\frac{\partial u_r}{\partial r}\cos\theta - \frac{\partial u_\theta}{\partial r}\sin\theta - (1-2\nu)\left(\frac{\partial u_r}{r\,\partial\theta} - \frac{u_\theta}{r}\right)\sin\theta\right] \\ &+ \frac{1}{\Phi^2}\left[-(3-4\nu)\frac{\partial u_\varphi}{\partial\varphi}\cos\theta - 2(1-\nu)(u_r\cos\theta - u_\theta\sin\theta)\cos\theta + (1-2\nu)\frac{\partial^2 u_r}{\partial\varphi^2}\right] \\ &- \frac{1}{\Phi^3}\frac{(1-2\nu)3b^2e^2\sin\varphi\cos\varphi}{a(1-e^2\sin^2\varphi)^{5/2}}\left(\frac{\partial u_r}{\partial\Phi} - u_\varphi\cos\theta\right) = 0, \end{aligned} \tag{4.2}$$

$$\frac{\partial^2 u_r}{r\,\partial r\,\partial\theta}+(3-4\nu)\frac{\partial u_r}{r^2\,\partial\theta}+(1-2\nu)\left(\frac{\partial^2 u_\theta}{\partial r^2}+\frac{\partial u_\theta}{r\,\partial r}-\frac{u_\theta}{r^2}\right)+2(1-\nu)\frac{\partial^2 u_\theta}{r^2\,\partial\theta^2}$$

$$+\frac{1}{\Phi}\left[\frac{\partial^2 u_\varphi}{r\,\partial\theta\,\partial\varphi}+\frac{\partial u_r}{r\,\partial\theta}\cos\theta-2(1-\nu)\left(\frac{\partial u_\theta}{r\,\partial\theta}+\frac{u_r}{r}\right)\sin\theta-\frac{u_\theta}{r}\cos\theta+(1-2\nu)\frac{\partial u_\theta}{\partial r}\cos\theta\right]$$

$$+\frac{1}{\Phi^2}\left[(1-2\nu)\frac{\partial^2 u_\theta}{\partial\varphi^2}+(3-4\nu)\frac{\partial u_\varphi}{\partial\varphi}\sin\theta+2(1-\nu)(u_r\cos\theta-u_\theta\sin\theta)\sin\theta\right]$$

$$-\frac{1}{\Phi^3}\frac{(1-2\nu)3b^2e^2\sin\varphi\cos\varphi}{a(1-e^2\sin^2\varphi)^{5/2}}\left(\frac{\partial u_\theta}{\partial\varphi}+u_\varphi\sin\theta\right)=0, \tag{4.3}$$

$$\frac{\partial^2 u_\varphi}{\partial r^2}+\frac{\partial u_\varphi}{r\,\partial r}+\frac{\partial^2 u_\varphi}{r^2\,\partial\theta^2}+\frac{1}{\Phi}\left[\frac{1}{1-2\nu}\left(\frac{\partial^2 u_r}{\partial r\,\partial\varphi}+\frac{\partial^2 u_\theta}{r\,\partial\theta\,\partial\varphi}+\frac{\partial u_r}{r\,\partial\varphi}\right)+\frac{\partial u_\varphi}{\partial r}\cos\theta-\frac{\partial u_\varphi}{r\,\partial\theta}\sin\theta\right]$$

$$+\frac{1}{\Phi^2}\left[\frac{2(1-\nu)}{1-2\nu}\frac{\partial^2 u_\varphi}{\partial\varphi^2}+\frac{3-4\nu}{1-2\nu}\frac{\partial u_r}{\partial\varphi}\cos\theta-\frac{3-4\nu}{1-2\nu}\frac{\partial u_\theta}{\partial\varphi}\sin\theta-\mu_\varphi\right]$$

$$-\frac{1}{\Phi^3}\frac{6e^2b^2(1-\nu)\sin\varphi\cos\varphi}{(1-2\nu)a(1-e^2\sin^2\varphi)^{5/2}}\left(\frac{\partial u_\varphi}{\partial\varphi}+ur\cos\theta-u_\theta\sin\theta\right)=0. \tag{4.4}$$

The boundary conditions are: when $\theta=\pm\pi$

$$\sigma_\theta=0,\qquad \sigma_{r\theta}=0,\qquad \sigma_{\theta\varphi}=0. \tag{4.5}$$

(b) *Eigenfunction expansion*

The governing eqs (4.2)–(4.4) are partial differential equations with variable coefficients. It is very difficult to solve them directly. As we are only interested in the stress–strain fields at crack tip, we can use the asymptotic technique.

Define the following dimensionless parameters:

$$\rho=\frac{r}{b^2/a},\qquad v_r=\frac{u_r}{b^2/a},\qquad v_\theta=\frac{u_\theta}{b^2/a},\qquad v_\varphi=\frac{u_\varphi}{b^2/a}.$$

Expand dimensionless displacements v_γ, v_θ, v_φ in double eigenexpansion series.

$$V_r=\sum_\lambda\sum_n\rho^{\lambda+n}a_n(\theta,\varphi;\lambda)=\sum_\lambda\rho^\lambda[a_0(\theta,\varphi;\lambda)+\rho a_1(\theta,\varphi;\lambda)+\cdots]$$

$$V_\theta=\sum_\lambda\sum_n\rho^{\lambda+n}b_n(\theta,\psi;\lambda)=\sum_\lambda\rho^\lambda[b_0(\theta,\varphi;\lambda)+\rho b_1(\theta,\varphi;\lambda)+\cdots]$$

$$V_\varphi=\sum_\lambda\sum_n\rho^{\lambda+n}c_n(\theta,\varphi;\lambda)=\sum_\lambda\rho^\lambda[c_0(\theta,\varphi;\lambda)+\rho c_1(\theta,\varphi;\lambda)+\cdots]. \tag{4.6}$$

Substituting eq. (4.6) into governing eqs (4.2)–(4.4) and boundary conditions eq. (4.5), compare the terms which have the same order of ρ. The asymptotic governing equations and boundary conditions could be found. From the governing equations and boundary conditions of zero order, the eigenfunction could be found.

$$\lambda=\pm n/2\qquad (n=0,1,2,\ldots). \tag{4.7}$$

From the condition of finite strain energy, the negative value should be neglected. From eq.

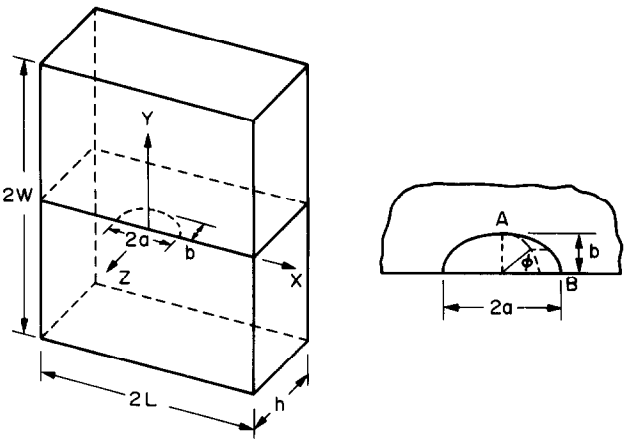

Fig. 4.2. A plate with surface crack.

(4.7), the double eigenexpansion series can be reduced to a single eigenexpansion series.

$$V_r = \sum_{n=0}^{\infty} \rho^{n/2} a_n(\theta, \varphi),$$

$$V_\theta = \sum_{n=0}^{\infty} \rho^{n/2} b_n(\theta, \varphi), \tag{4.8}$$

$$V_\varphi = \sum_{n=0}^{\infty} \rho^{n/2} c_n(\theta, \varphi).$$

Substituting eq. (4.8) into eqs (4.2)–(4.4) and eq. (4.5), the asymptotic governing equations and boundary conditions could be found. With the asymptotic solution of displacements v_γ, v_θ and v_φ known, the stress–strain fields at crack tip could be obtained[40].

(c) *The calculation of stress intensity factors in a plate with surface crack*

In ref. [40], based on the stress–strain fields at crack tip obtained, a three dimensional high order special element is established to calculate the stress intensity factors in a plate with surface crack.

Comparison of authors' solution with Newman and Raju's. In ref. [40] Newman and Raju proposed the expression of stress intensity factor in a plate with surface crack.

$$K_I = \sigma_1 \sqrt{\frac{\pi b}{\alpha}} F_i\left(\frac{b}{h}, \frac{b}{a}, \frac{a}{L}, \phi\right) \tag{4.9}$$

where a, b denote the major semi-axis and minor semi-axis of the ellipse, respectively. $2L$ denotes length of plate, $2w$ denotes width of plate and h denotes plate thickness. $F_i(b/h, b/a, a/L, \phi)$ denotes dimensionless stress intensity factor. Q denotes the shape factor for an ellipse. A useful approximation for Q is

$$Q = 1 + 1.46\left(\frac{b}{a}\right)^{1.65}. \tag{4.10}$$

In ref. [40], the values for $F_i(b/h, b/a, a/L, \phi)$, the dimensionless stress intensity factors, were calculated for $a/b = 0.6$, $b/h = 0.6$, $a/L = 0.2$, $a/w = 0.2$, $\nu = 0.3$ case. The mesh is shown in Fig. 4.3. The number of freedoms we adopted is equal to 838, and almost equals to $\frac{1}{10}$ of that Newman and Raju adopted. The results are shown in Fig. 4.4(a, b) and compares with that in ref.

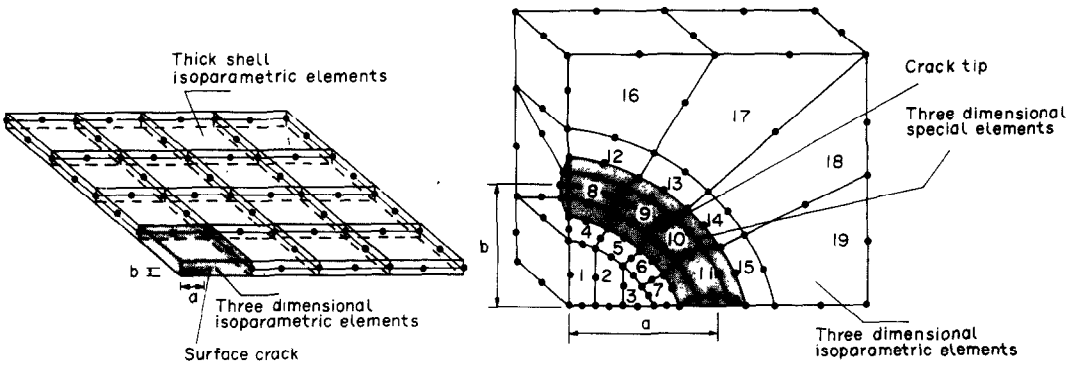

Fig. 4.3. The finite element mesh.

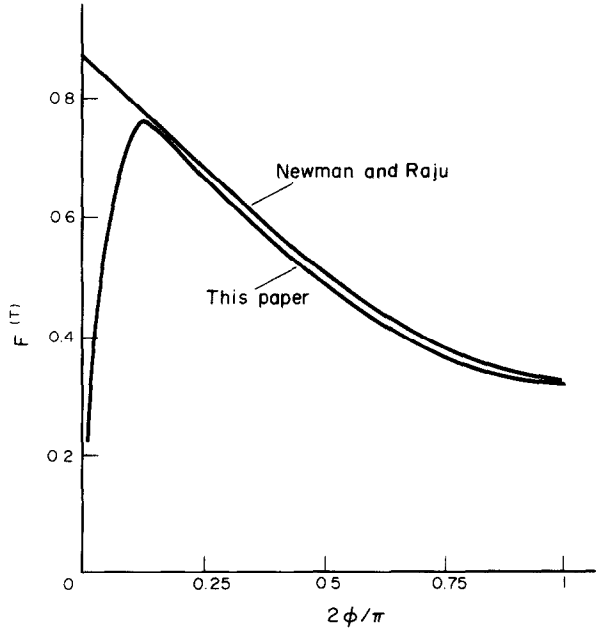

(a)

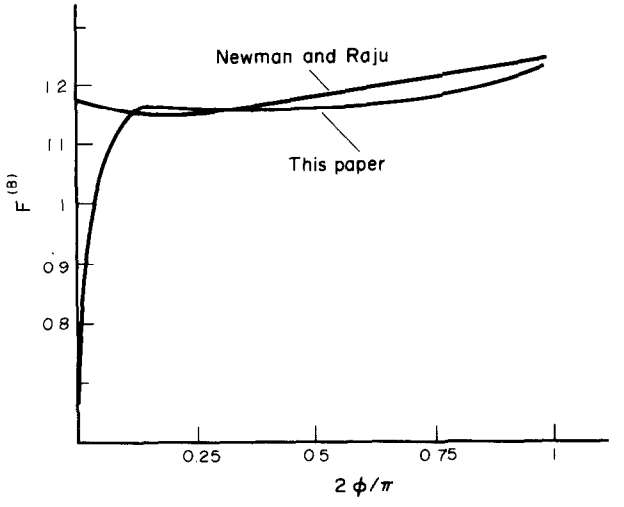

(b)

Fig. 4.4. (a) Comparison of authors' solution with others (Tension). (b) Comparison of authors' solution with others (Bending).

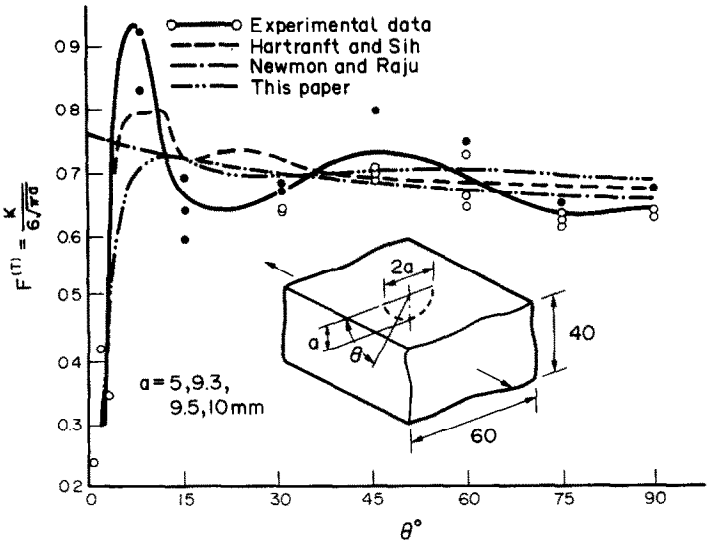

(a)

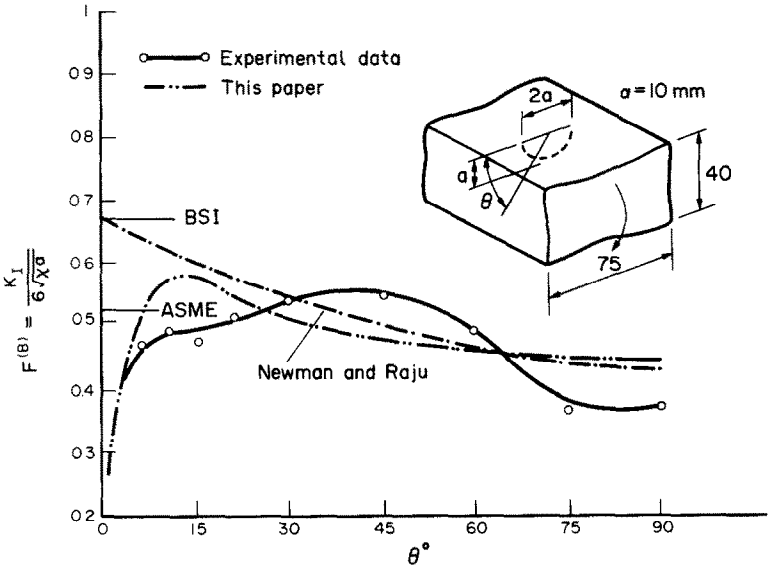

(b)

Fig. 4.5. (a) Comparison of authors' solution with experimental data (Tension). (b) Comparison of authors' solution with experimental data (Bending).

[37]. It is shown that, at the point A, the end of minor axis, the difference between authors' results and Newman and Raju's, for tension is 0.37%, for bending is 1.81%.

According to the author's results, the stress intensity factor dropped dramatically near the plane surface. Meanwhile, in ref. [39] photo-elastic experimental data show that there is a thin boundary layer near plate surface, the stress intensity factor drops off rapidly but is not equal to zero. The author's results compare favourably with the experimental data (Fig. 4.5a, b).

Variation of stress intensity factors with width of plate. In ref. [40], the dimensionless stress intensity factors were calculated for $b/a = 0.6$ case with $a/L = 0.05$, 0.1, 0.15, 0.2, 0.25, 0.3, 0.4. The results are shown in Fig. 4.6(a, b).

Variation of stress intensity factors with plate thickness. In ref. [40], the dimensionless stress intensity factors were calculated for $b/a = 0.6$, $a/L = 0.2$, $a/w = 0.2$ case with $b/h = 0.2$, 0.4, 0.6, 0.75. The results are shown in Fig. 4.7(a, b). Meanwhile, the results of 14 investigators' work were collected, the authors' results are included as well (See Fig. 4.8).

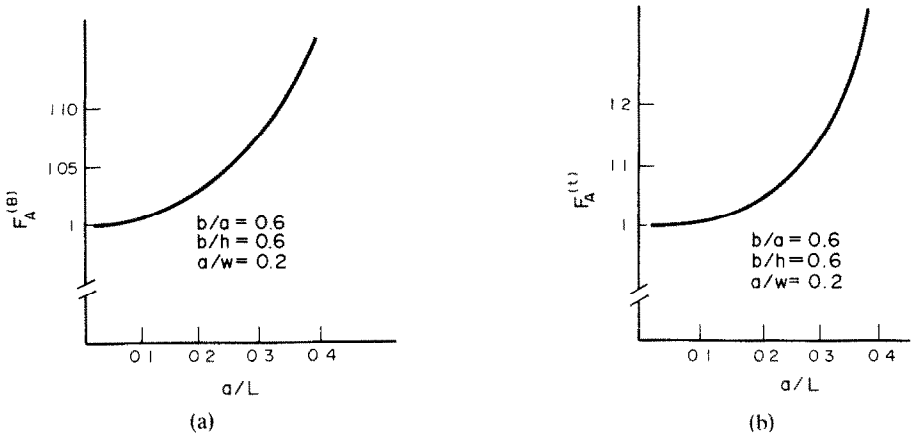

Fig. 4.6. (a) Variation of stress intensity factors with plate width (Tension). (b) Variation of stress intensity factors with plate width (Bending).

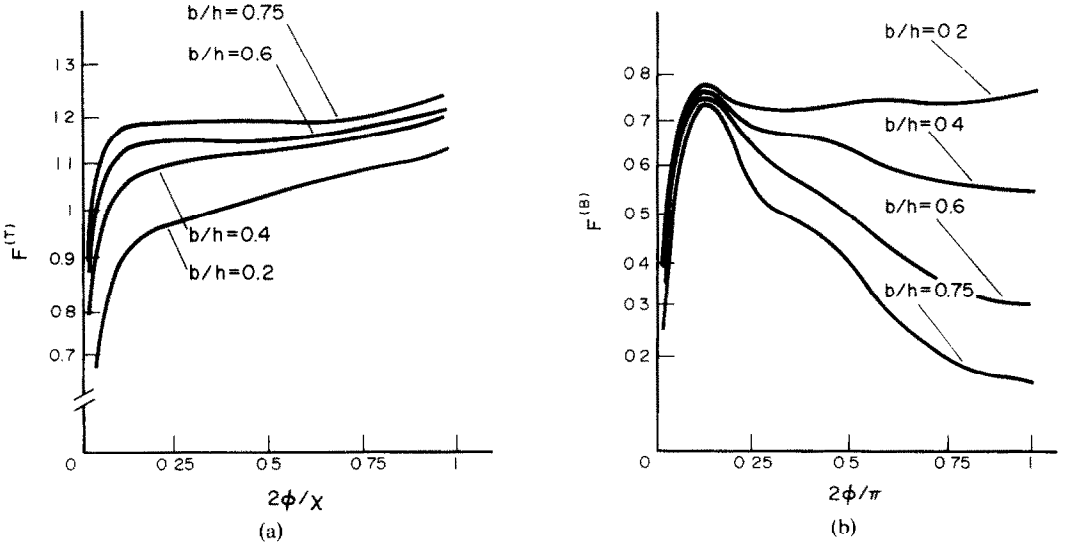

Fig. 4.7. (a) Variation of stress intensity factors with plate thickness (Tension). (b) Variation of stress intensity factors with plate thickness (Bending).

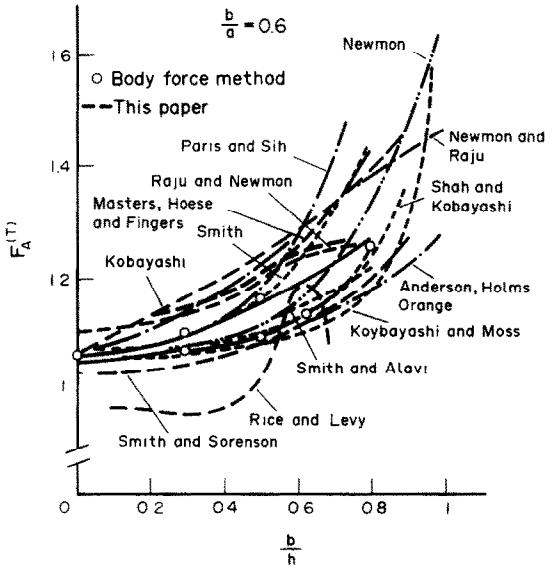

Fig. 4.8. Comparison of authors' solution with others.

5. CONCLUSION

(1) In this paper so-called "local-global analysis" is used systematically for fracture analysis in cracked plates, shells and three dimensional bodies with surface crack. The general solutions of stress–strain fields at crack tip including mode I, mode II and mode III in Reissner's plate, shell and three dimensional bodies were proposed for the first time. Similar to the Williams expansion in plane fracture problem, they reveal the mechanical behavior near the crack tip and provide a better foundation for numerical fracture analysis. The analytical method for plane fracture problem, such as variational method, asymptotic method and finite element method, could be adopted for cracked plate, shell and three dimensional body fracture analysis.

(2) Based on the stress–strain fields obtained, several kinds of high-order special elements were proposed to substitute the dense mesh near the crack. Meanwhile, since more accurate displacement modes are used, the calculation accuracy could be improved.

(3) For cracked plate and shell fracture analysis, the Reissner's theory was used to avoid the defect of classical theory. There is obvious difference between the calculation results by using different theories.

(4) The stress intensity factors in finite size plate and shell for symmetric and anti-symmetric cases are calculated with higher accuracy. The variation of stress intensity factors with geometrical parameters was investigated.

(5) A special coordinate transformation is proposed to search for the stress–strain fields at crack tip in three dimensional body with surface crack. This method is not only suitable for semi-elliptical crack, but also suitable for arbitrary crack.

(6) The stress intensity factors in a finite size plate with surface crack were calculated. Compared with Newman and Raju's results, the error is less than 5% except in the region near plate surface. The number of freedoms we adopted is only $\frac{1}{10}$ of that Newman and Raju adopted. On a Univac 1100 computer, it takes only 18 minutes to finish a three dimensional finite element fracture analysis.

REFERENCES

[1] M. L. Williams, *J. appl. Mech.* **28**, 78–82 (1961).
[2] G. C. Sih and P. C. Paris, *J. appl. Mech.* **29**, 306–310 (1962).
[3] J. K. Knowles and N. M. Wang, *J. Math. Phys.* **39**, 223–236 (1960).
[4] R. J. Hartranft and G. C. Sih, *J. Math. Phys.* **47** (1968).
[5] M. V. V. Murthy, K. N. Raju and S. Viswanath, *Int. J. Fracture* **17**, 537–552 (1981).
[6] N. M. Wang, *J. Math. Phys.* **47**, 371–390 (1968).
[7] F. Delale and F. Erdogan, *J. appl. Mech.* **46**, 3 (1979).
[8] G. Yagawa, *Int. J. numer. Meth. Engng* **14**, 5 (1979).
[9] R. S. Barsoum, *Int. J. numer. Meth. Engng* **10**, 551–564 (1976).
[10] H. C. Rhee and S. N. Atluri, *Int. J. numer. Meth. Engng* **18**, 259–261 (1982).
[11] Li Ying Zhi and Liu Chuntu, *Acta Mech. Sinica*, **4**, 366–375 (1983).
[12] Liu Chuntu, *Acta Mech. Solida Sinica* **3**, 441–448 (1983).
[13] Liu Chuntu and Li YingZhi, *Proc. ICF Int. Symp. Fracture Mech.* (Beijing, 1983).
[14] Li YingZhi and Liu Chuntu, *Proc. Int. Conf. Computational Mech.*, (Tokyo, ICCM86).
[15] Liu Chuntu, Hu Huaichang, *J. Taiyuan Heavy Mech. Inst.*, **2** (1985).
[16] E. S. Folias, *Int. J. Fracture Mech.* **1**, 20–44 (1965).
[17] F. Erdogan and J. Kibler, *Int. J. Fracture Mech.* **5**, 229–237 (1969).
[18] G. C. Sih and P. S. Dobreff, *Glasgow Math. J.* **12**, 65–88 (1971).
[19] P. M. Naghdi, *Q. appl. Math.* **54**, 369–380 (1957).
[20] G. C. Sih and H. C. Hagendorf, *Mechanics of Fracture* (Edited by G. C. Sih), Vol. 3 (1973).
[21] F. Delale and F. Erdogan, *Int. J. Solid Struct.* **15**, 907–926 (1979).
[22] F. Delale, *Int. J. Engng Sci.* **20**, 1325–1347 (1982).
[23] Liu Chuntu and Li Yingzhi, *Proc. ICF6* (Edited by S. R. Valluri *et al.*), New Delhi, Vol. 2, pp. 791–801 (1984).
[24] Li Chuntu, Wu Xijia and Li YingZhi, *Proc. 4th Chinese Nat. Conf. Fracture Mech.*, Xian (1985).
[25] Wu Xijia, Liu Chuntu, *Proc. 4th Chinese Nat. Conf. Fracture Mech.*, Xian (1985).
[26] G. R. Irwin, *J. appl. Mech.* **29**, 651–654 (1962).
[27] F. W. Smith, Stresses near a Semicircular Edge Crack. Ph.D. thesis, Univ. of Washington (1966).
[28] F. W. Smith and M. J. Alavi, *J. Engng Fracture Mech.* **1** (1969).
[29] R. W. Thresher and F. W. Smith, *J. appl. Mech.* **39**, 1 (1972).
[30] F. W. Smith, *Int. J. Fracture* **12**, 1 (1976).
[31] J. R. Rice and N. Levy, *J. appl. Mech.* **39**, 185 (1972).
[32] H. Nisitani, *Mechanics of Fracture* (Editied by G. C. Sih), Vol. 5.
[33] M. Isida, H. Noguchi and T. Yoshida, *Int. J. Fracture* **26**, 157–188 (1984).

[34] J. L. Swedlow (ed.), *The Surface Crack: Physical Problems and Computational Solutions* (1972).
[35] J. C. Newman, *ASTM STP* **687**, 16–24 (1979).
[36] I. S. Raju and J. C. Newman, NASA TND-8414 (1977).
[37] J. C. Newman and I. S. Raju, NASA TP-1578 (1979).
[38] *Annual book of ASTM Standards*. ASTM (1983).
[39] C. Ruiz and J. Epstein, *On the Variation of the Stress Intensity Factor Along the Front of a Surface Flaw*. Oxford OX1 3PJ.
[40] Li YingZhi, The Stress-Strain Fields at Crack Tip in Cracked Plate, Three Dimensional Body with Surface Crack and the Calculation of Stress Intensity Factors. Ph.D. thesis, Institute of Mechanics, Chinese Academy of Sciences (1986).